Supplementary Information

Ultra-thin Patchy Polymer-Coated Graphene Oxide as a Novel Anticancer Drug Carrier

Vien T. Huynh,[a,b] Duc Nguyen,[a,b] Liwen Zhu,[a,b] Nguyen T. H. Pham,[a,b] Pramith Priyananda,[a] and Brian S. Hawkett.*[a,b]

[a] Key Centre for Polymers and Colloids, School of Chemistry F11,

The University of Sydney, NSW 2006, Australia

[b] University of Sydney Nano Institute, The University of Sydney, NSW 2006, Australia

1. Synthesis of 2-[(butylsulfanyl)carbonothioyl] sulfanyl propanoic acid (BuPATTC)

BuPATTC RAFT agent was synthesised as previously described.[1] Briefly, a mixture of butanethiol (154.6g, 1.718 mole) and water (225 mL) in a 2 L flanged RBF under a stream of nitrogen was vigorously stirred in an ice bath and cooled to <10 °C. 50% sodium hydroxide solution (137.4 g, 1.718 mole) was added rapidly by a syringe and the currently clear homogeneous solution was stirred in the ice bath for 30 min before 2-bromopropionic acid was added slowly to give a cloudy burnt orange coloured reaction. This was re-cooled to below room temperature over 0.5h, and then treated with 50% sodium hydroxide. ^{1}H-NMR (300 MHz, $CDCl_3$, 25 °C) δ (ppm) = 10.50-8.40 (1H, $CH_3CH_2CH_2CH_2SCH(S)SCH(CH_3)$**C(O)OH**), 4.95-4.83 (1H, $CH_2SCH(S)S$**CH**$(CH_3)C$),

3.46-3.32 (2H, $CH_2CH_2\mathbf{CH_2}SCH(S)SCH$), 1.78-1.65 (2H, $CH_3CH_2\mathbf{CH_2}CH_2SCH$), 1.70-1.60 (3H, $CH_2SCH(S)SCH(\mathbf{CH_3})C(O)OH$), 1.54-1.36 (2H, $CH_3\mathbf{CH_2}CH_2CH_2SCH$), 1.05-0.90 (3H, $\mathbf{CH_3}CH_2CH_2CH_2SCH$).

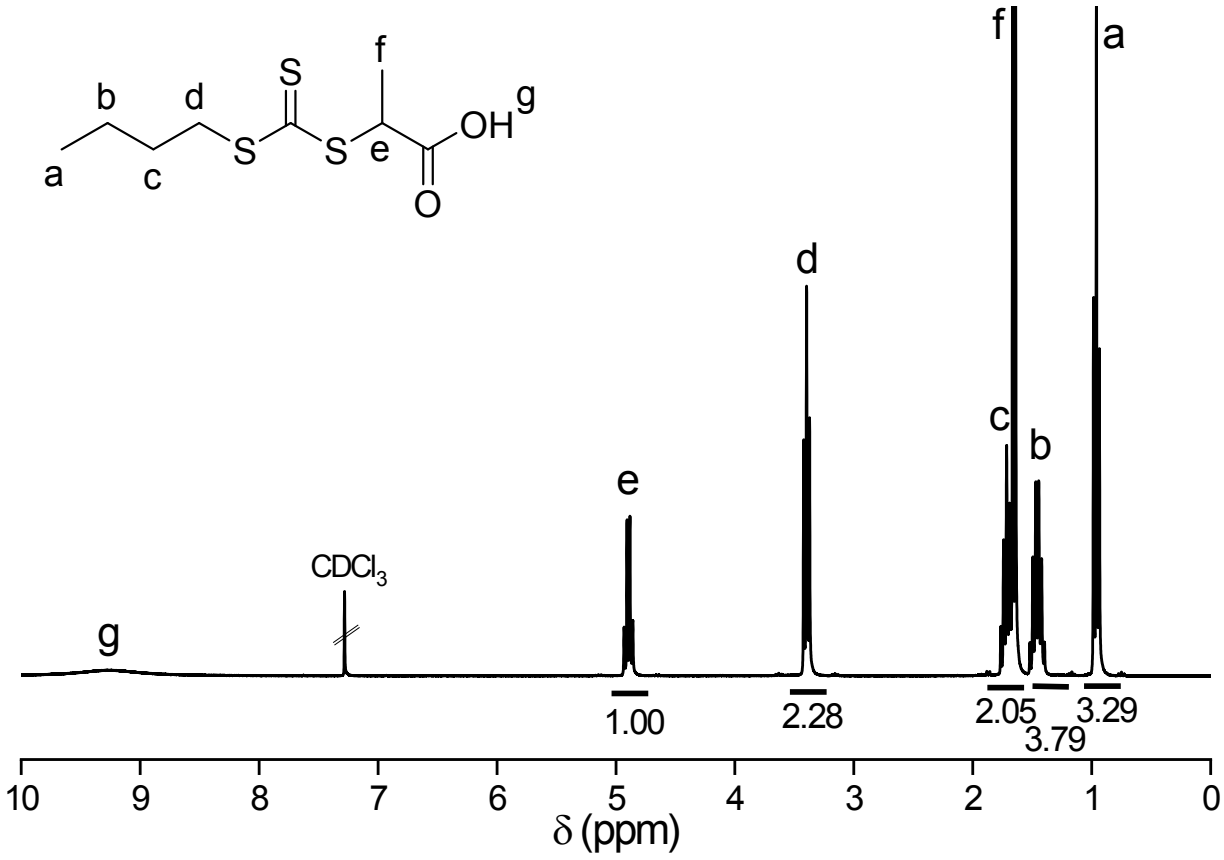

Figure S1:[1]H-NMR spectrum of BuPATTC RAFT agent was performed in deuterated chloroform

2. Synthesis of macro-RAFT copolymer, BuPATTC-(BA_4-*stat*-AA_9-*stat*-StS_5)

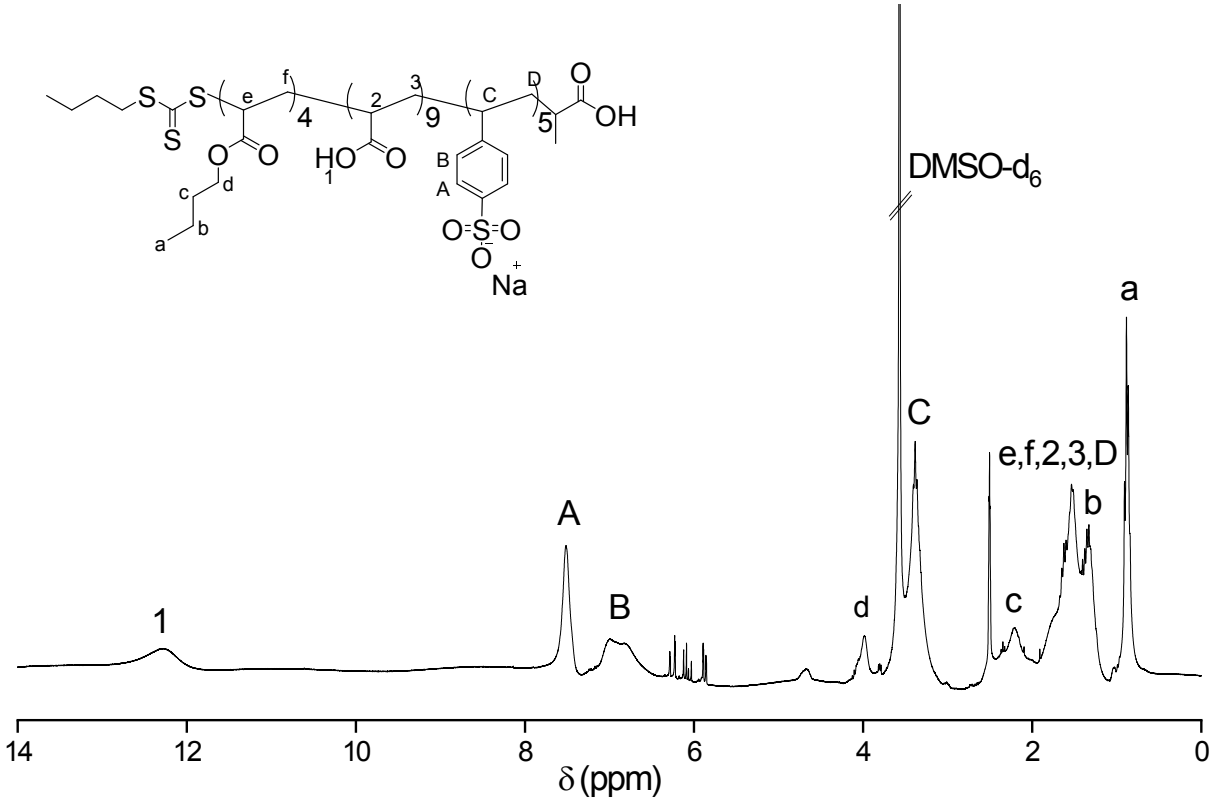

Figure S2: ^{1}H-NMR of BuPATTC-(BA_4-*stat*-AA_9-*stat*-StS_5)

3. Zeta potential of GO versus pH

The zeta potential results shown in Figure S3 clearly revealed the GO surface became increasingly negatively charged with increasing pH from −15 to −40 mV corresponding to a pH of 3 and 9, respectively. However, it was observed to level off when the pH exceeded 8, indicating the complete deprotonation of the carboxylic acid groups.

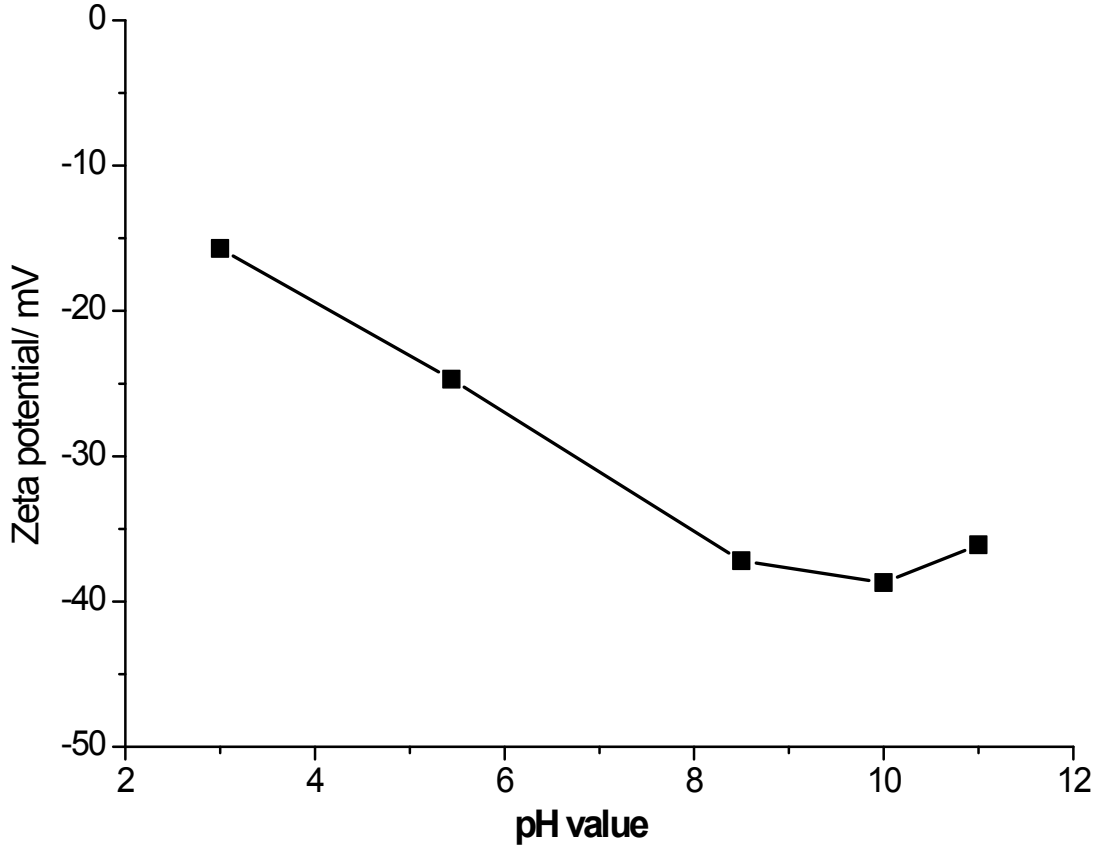

Figure S3: Zeta potential of GO dispersion as a function of pH

4. Synthesis of poly(MMA-co-BA) particle latex using Amphiphilic macro-RAFT copolymers as stabilisers

Gel permeation chromatography (GPC) was implemented using UFLC Shimadzu Prominence system comprising a DGU-20A degasser, a LC-20AD pump, a SIL-20A HT automatic injector, a CTO-20A column oven, a RID-10A refractive index detector, a RF-20A fluorescence detector and a SPD-M20A Diode array detector Shimadzu UV/vis detector. A 50 x 7.8 mm guard column and two 300 x 7.8 mm linear columns (104 and 105 Å pore size, 5 μm particle size) were used for the analyses. *N,N'*-dimethylacetamide (DMAc) (HPLC grade, 0.05% w/v of 2,6-dibutyl-4-methylphenol (BHT), 0.03% w/v of LiBr) with a flow rate of 1 mL min^{-1} and a constant temperature

of 50 °C was used as the mobile phase with an injection volume of 25 µL. The unit was calibrated using commercially available linear poly(methyl methacrylate) standards (0.5- 1000 kDa, Polymer Laboratories). The samples (4 mg mL^{-1}) were dissolved in DMAc and filtered through 0.45 µm PTFE filters. It is noted that the polymer latex was neutralised using HCl 0.2 M prior to drying and subsequently dissolving in the DMAc for GPC sample preparation. Carboxylic groups in both the macro-RAFT copolymer and the resulting polymer latex were methylated using (trimethylsilyl) diazomethane prior to the sample preparation.

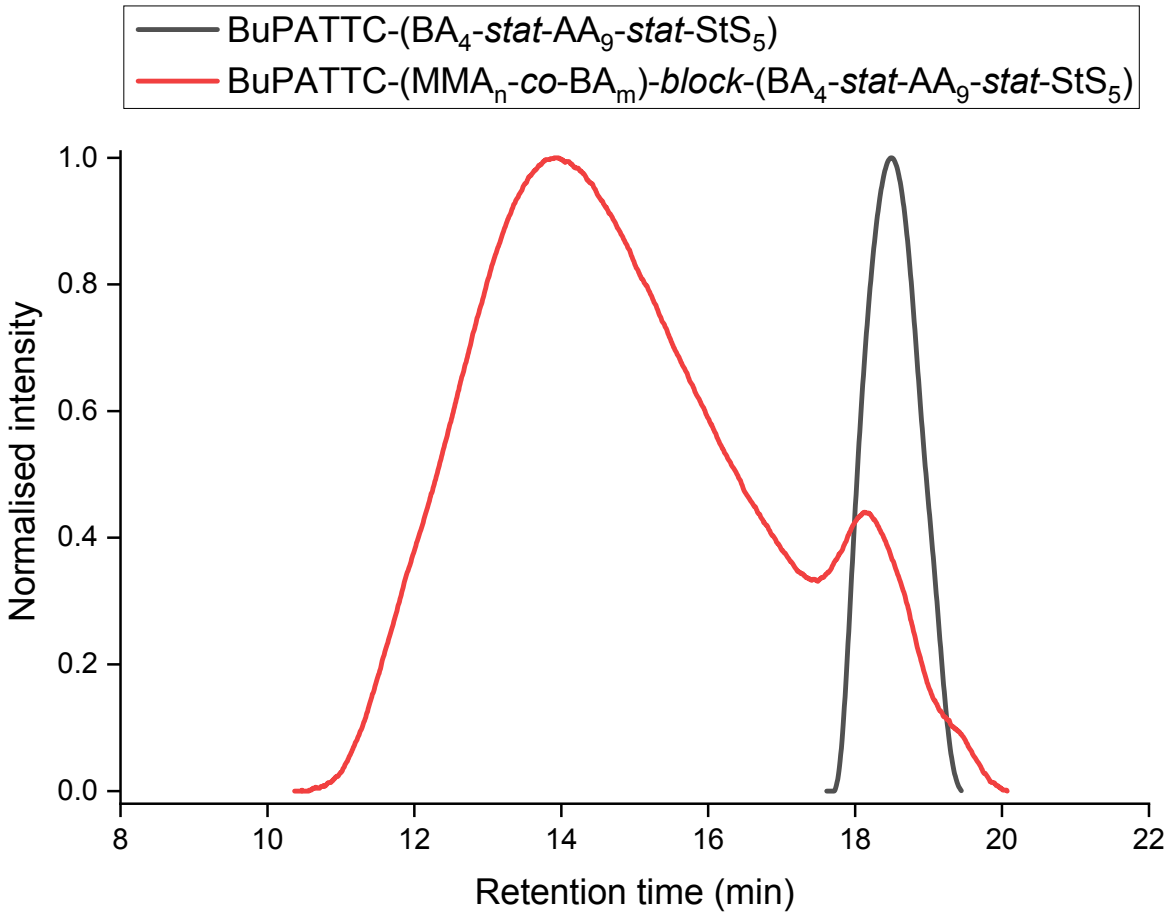

Figure S4: GPC traces of BuPATTC-(BA_4-*stat*-AA_9-*stat*-StS_5) and BuPATTC-(MMA_n-*co*-BA_m)-*block*-(BA_4-*stat*-AA_9-*stat*-StS_5).

GPC measurements of molecular weight were carried out on the macro-RAFT copolymer, BuPATTC-(BA_4-*stat*-AA_9-*stat*-StS_5) and the total polymer present in the reacting system, BuPATTC-(MMA_n-*co*-BA_m)-*block*-(BA_4-*stat*-AA_9-*stat*-StS_5). Figure S4 shows that there was a significant shift in molecular weight distribution as the starve-fed polymerisation progressed, demonstrating that the polymer grown was living. A shoulder peak was also observed, at similar retention times to the original macro-RAFT copolymer. This could be because some highly labile macro-RAFT copolymers did not undergo chain extension in the aqueous phase as discussed in our previous work.[2]

5. Dispersion of graphene oxide in prepared polymer nanoparticles

It is worth confirming the observed PPC-GO morphology to make sure that it was not an artefact of drying the sample. Similar size polymer latex particles with the same surface chemistry were prepared by carrying out *ab initio* emulsion polymerisation via RAFT-controlled self-assembly. The particles were then used to disperse the GO using sonication prior to TEM assessment.

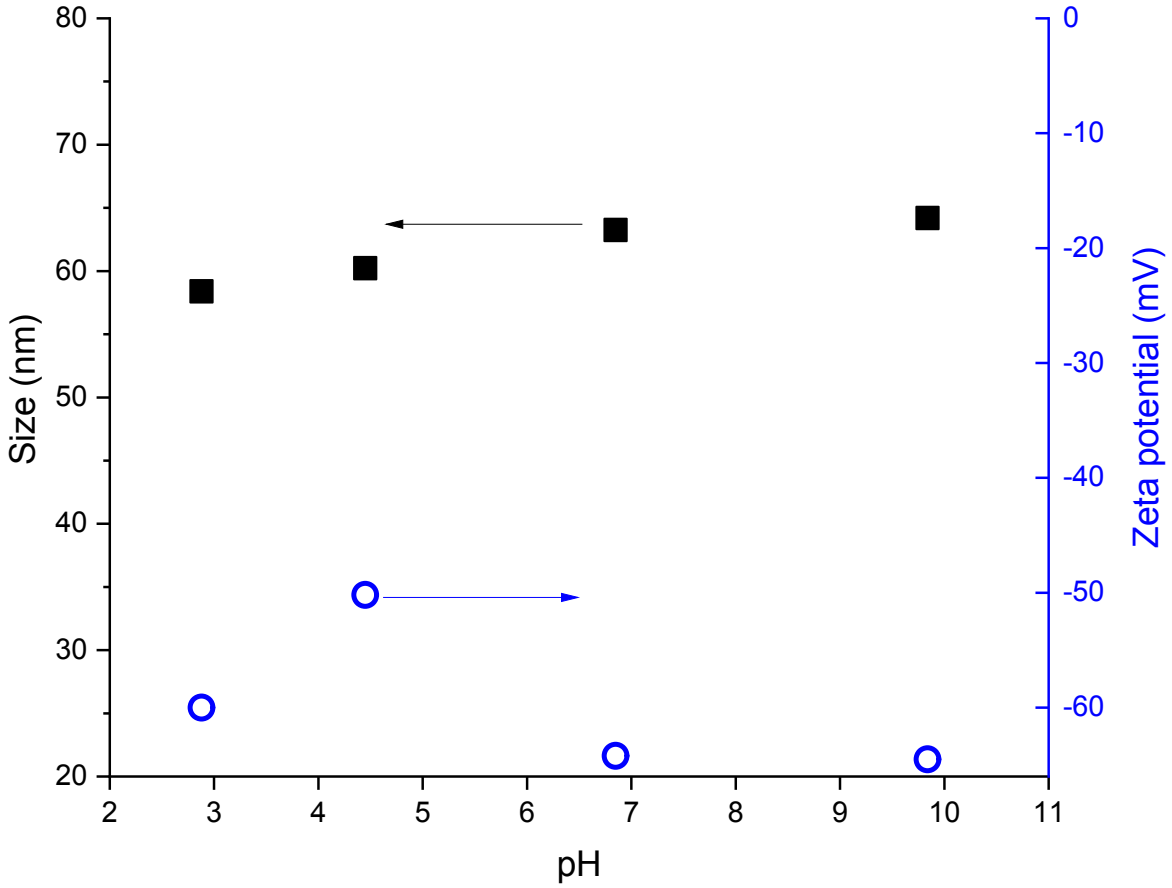

Figure S5: Size and zeta potential of the polymer latex particles prepared by *ab initio* emulsion polymerisation via RAFT-controlled self-assembly at different pH values.

6. AFM analysis of PPC-GO with various monomer/GO ratios

Table S1: Average height of polymer bumps and nodes on the partial polymer-coated GO at different monomer feeding concentrations. The reported height is an average of the heights of 20 points on sample surface.

Sample ID	**Macro-RAFT copolymer concentration (g/L)**	**Mass ratio of MMA/BA (10/1, w/w)/GO**	**Average height of GO sheet (nm)**	**Average height of polymer bumps or nodes (nm)**
VH440072-0	1.43	0	1.4	0
VH440072-1	1.43	0	2	0
VH440072-2	1.43	10	1.4	10
VH440072-3	1.43	35	1.4	22
VH440072-4	1.43	70	N/A	48
VH440072-5	1.43	140	N/A	67

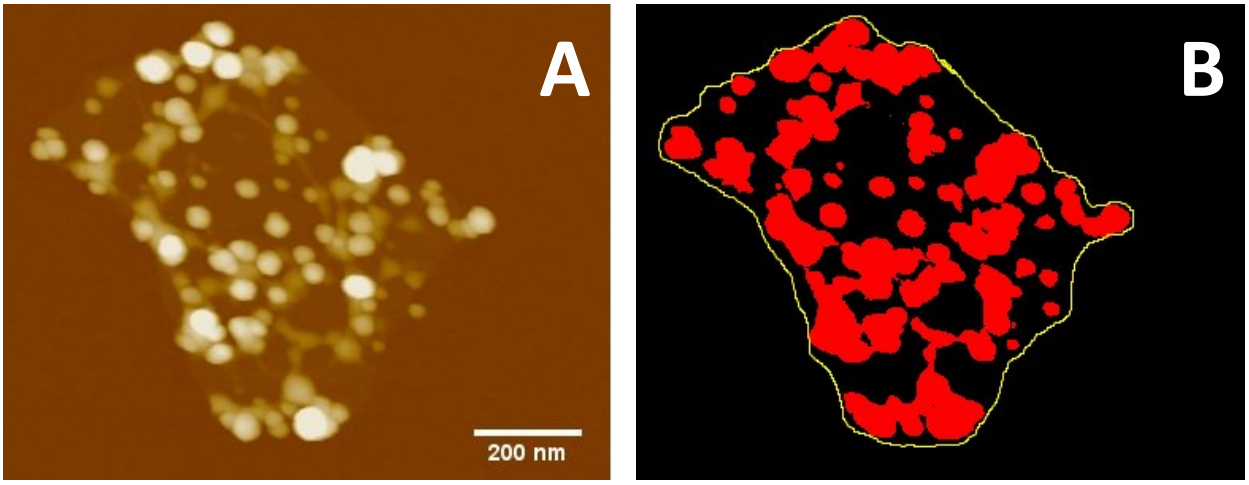

Figure S6: AFM microstructures showing calculation of polymer coverage percentage using ImageJ software: (A) original AFM of PPC-GO with Mass ratio of MMA/BA (10/1, w/w)/GO = 35 and (B) polymer coverage percentage estimated by ImageJ of the similar polymer-coated GO. The polymer coverage was found to be around 43%.

7. Reduction of GO using *L*-AA

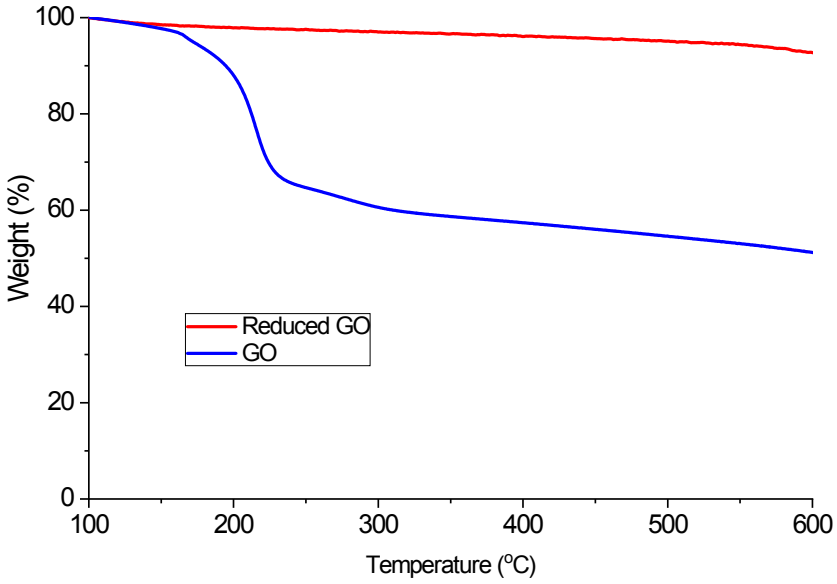

Figure S7: TGA of the bare GO and the rGO prepared by reducing GO with L-AA

8. Stability of Dox-PPC-GO

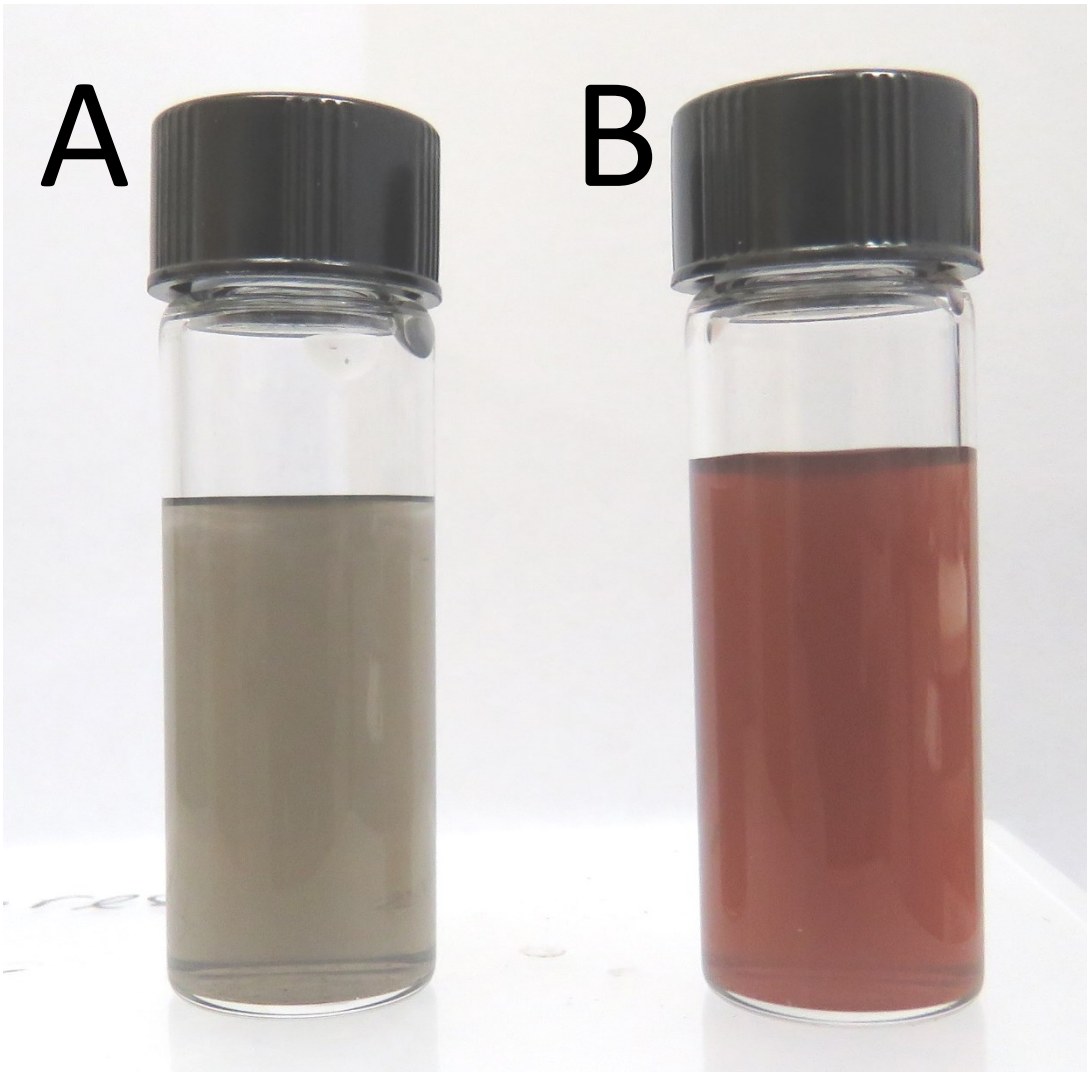

Figure S8: Dispersions of (A) PPC-GO and (B) Dox-PPC-GO in DI water.

Notes and references

1. C. J. Ferguson, R. J. Hughes, D. Nguyen, B. T. T. Pham, R. G. Gilbert, A. K. Serelis, C. H. Such and B. S. Hawkett, *Macromolecules*, 2005, **38**, 2191-2204.

2. D. Nguyen, H. S. Zondanos, J. M. Farrugia, A. K. Serelis, C. H. Such and B. S. Hawkett, *Langmuir*, 2008, **24**, 2140-2150.